Adv Syst Sci Appl 2024; **02**; 116-132
Published online at https://ijassa.ipu.ru.

Adjusting the Parameters of a PID Controller with an Asymmetric Fuzzy Algorithm for an Automotive Suspension System

Tuan Anh Nguyen

Thuyloi University, Hanoi, Vietnam

Abstract: A suspension system plays a crucial role in ensuring the smoothness of a car when traveling on roads. This paper proposes using the active suspension system equipped with a hydraulic actuator to replace a conventional passive suspension. Unlike previous publications, this study uses a Hybrid proportional-integral-derivative (PID) algorithm, combining a conventional PID controller and a fuzzy solution with two distinct inputs. The coefficients of the PID controller are flexibly adjusted by the fuzzy algorithm. Therefore, it can more respond to complex motion conditions. Calculations are performed with the MATLAB-Simulink software for four specific cases. According to the research findings, the maximum and root mean square (RMS) values of vehicle body acceleration and displacement significantly decrease when applying the hybrid algorithm to the active suspension system. In the last case, these values are only 16.69% and 36.90% when comparing Fuzzy PID and Passive situations. In general, the smoothness of the sprung mass can be guaranteed in all survey cases.

Keywords: Active suspension system, hybrid PID algorithm, Fuzzy PID controller, dynamics vehicle.

1. INTRODUCTION

Automotive vibration is an exciting topic that attracts many researchers. Car vibrations have an essential influence on the stability and smoothness of the vehicle when traveling. Suspension systems are fitted on cars and other vehicles to control their vibration [1]. A conventional suspension system, also known as a passive suspension (mechanical suspension), has three essential components: metal springs, dampers, and lever arms or multi-link bars. This simple suspension system is commonly used on most vehicles today. Its cost is relatively low, but its efficiency is not high. Therefore, the components of the passive suspension system should be improved to enhance the quality of the system. In [2], Yoon et al. came up with the idea of using electromagnetic dampers instead of conventional passive dampers. For this suspension system, the damper's force could be controlled by an electric current applied to electrodes inside the shock absorber. According to Zheo et al. [3], spring stiffness could be controlled by utilizing air balloons instead of metal springs. The suspension system performance could be improved by using the above two solutions. However, they only partially met requirements regarding stability and smoothness. Pan and Sun proposed using the active suspension system to ensure the criteria of road holding and ride comfort [4]. Unlike air spring and electromagnetic damping suspension, the active suspension system was equipped with an additional hydraulic actuator that might generate large impact forces, according to Kilicaslan [5]. The performance of active suspension systems is often higher than other systems.

Many studies related to suspension control have been published in a past decade. In [6], Jeong et al. designed the linear quadratic (LQ) controller for the suspension model of 2 degrees of freedom (DOFs) and 7 DOFs. This algorithm aimed to minimize the cost function of the controller. Algorithm parameters could be determined using various solutions, such as ant

colony optimization [7] or in-loop solution [8]. A Gaussian filter was used to limit the noise from the outside; therefore, it became the LQG controller [9].

When considering the oscillating system to be nonlinear, Wang et al. applied a robust predictive control method for a suspension system with a spatial model [10]. To improve the stability of nonlinear control algorithms, Li et al. used H_∞ nonfragile optimization method, which considered the delay of the hydraulic actuator [11]. Using the sliding mode control (SMC) algorithm was a suitable solution for nonlinear systems. In [12], Ovalle et al. introduced a continuous sliding mode controller for the quarter model. For uncertain systems [13], retrofitting observers was necessary [14, 15]. The SMC algorithm might bring high performance to the system, but chattering phenomena still existed when applying this algorithm to oscillating systems. In [16], Nguyen showed the in-loop method to define the parameters for the sliding mode controller. This method was implemented based on minimizing the RMS values of acceleration and displacement. A newer improvement was shown in [17], where the optimization considered the oscillations' phase difference. In addition, the combination of the SMC algorithm and the fuzzy algorithm could help limit chattering in many situations, according to Golouje and Abtahi [18] and Shaer et al. [19].

Recently, fuzzy control algorithms have been widely applied in many studies on active suspension control [20, 21]. In [22], Mustafa et al. used a fuzzy algorithm with three membership functions of triangular shape. Each function had five steps: negative large (NL), negative small (NS), zero (ZE), positive small (PS), and positive large (PL). Meanwhile, Wang et al. used only a simple membership function related to error $e(t)$ for the fuzzy controller of the suspension system [23]. The membership functions of a fuzzy system could be the same or different, symmetric or asymmetric [24]. This depended on the designer's point of view. Fuzzy controllers could be optimized using particle swam optimization (PSO) algorithms, which describe the properties of animals such as cuckoos [25], bees [26], etc. In addition, combining fuzzy algorithms and other algorithms could help improve the controller's efficiency [27, 28].

The use of fuzzy algorithms to adjust the parameters of the PID controller is a fascinating idea that has attracted more interest from many researchers. Unlike optimization methods like PSO [7, 25, 26] or in-loop [8, 16, 17], fuzzy algorithms could generate dynamic changes in different controls instead of just finding a specific optimal value [29]. In [30], Nguyen and Nguyen used a simple fuzzy algorithm with one input. The input signal was the system's error after it had been derivative twice, while the output signal was the value of the coefficients k_P and k_I of the PI controller. In [31], Khodadadi and Hamid Ghadiri used a fuzzy controller with two inputs: velocity and acceleration. The membership functions used in [31] were triangular and trapezoidal. Fuzzy rules were often chosen symmetrically and described through fuzzy surfaces [32, 33]. Constructing fuzzy rules and membership functions significantly depended on the designer's experience. In some cases, the process of determining these rules could be derived from other algorithms [34, 35]. In general, the active suspension system might respond well to changing external conditions once the PID controller parameters were flexibly adjusted by the fuzzy algorithm [36-38]. This was proven through simulation and experiment [37, 39].

Based on the above evaluation and analysis, we propose to use the PID algorithm to control the active suspension system. A new fuzzy algorithm dynamically fine-tunes controller parameters; hence, it is called hybrid PID control. Fuzzy algorithms in previous studies often only had symmetric or straightforward forms [30-33]. Therefore, it could only provide ride comfort under certain conditions. In this work, an asymmetric fuzzy algorithm is designed as an alternative to conventional fuzzy algorithms. This helps to ensure the car's smoothness when oscillating without affecting other problems. This is a new contribution to the paper, demonstrated through simulation results. This paper content is divided into four parts: introduction, mathematical model, result and discussion, and conclusion.

2. MATHEMATICAL MODEL

The mathematical model of the system and the control method are presented in this section.

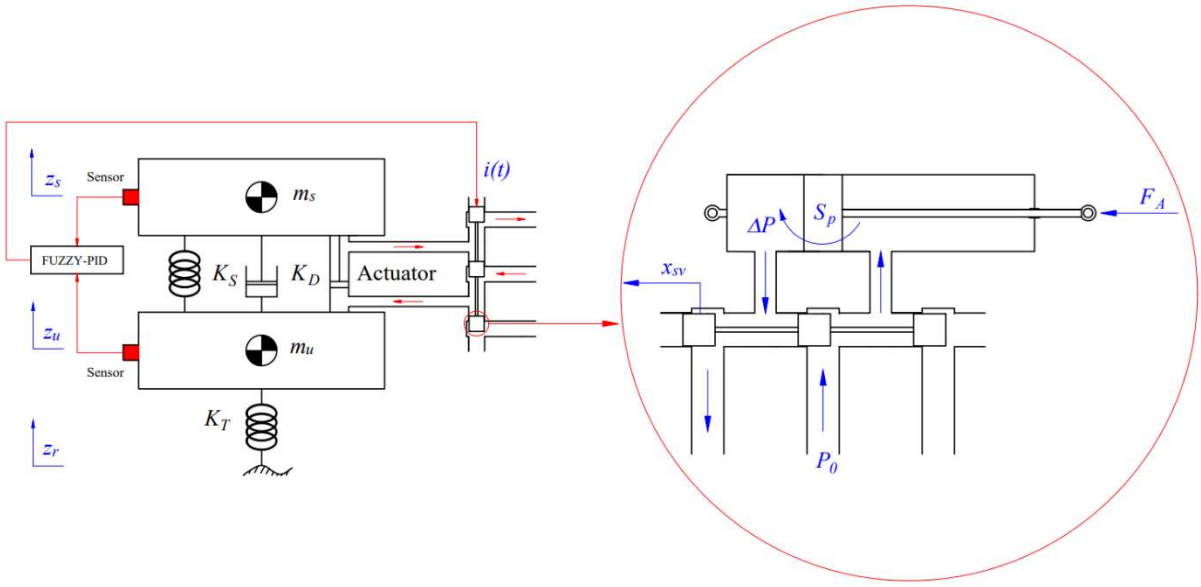

Fig. 1. Dynamic models.

Consider a suspension dynamics model, as shown in Figure 1. This is called a quarter model, with two masses, m_s and m_u, corresponding to z_s and z_u displacements. Applying d'Alembert's principle, we can obtain the following equations:

$$F_{is} - F_S - F_D - F_A = 0, \tag{1}$$

$$F_{iu} + F_S + F_D + F_A - F_T = 0, \tag{2}$$

where:

F_{is} – Inertia force of spung mass, N:

$$F_{is} = m_s \times \ddot{z}_s; \tag{3}$$

F_{iu} – Inertia force of unsprung mass, N:

$$F_{iu} = m_u \times \ddot{z}_u; \tag{4}$$

F_S – Spring force, N:

$$F_S = K_S \times (z_u - z_s); \tag{5}$$

F_D – Damping force, N:

$$F_D = K_D \times (\dot{z}_u - \dot{z}_s); \tag{6}$$

F_T – Tire force, N:

$$F_T = K_T \times (z_r - z_u); \tag{7}$$

F_A – Actuator force, N;
K_S – Spring coefficient, N/m;
K_D – Damping coefficient, Ns/m;
K_T – Tire coefficient, N/m;
m_s – Sprung mass, kg;
m_u – Unsprung mass, kg;
z_s – Sprung mass displacement, m;
z_u – Unsprung mass, m.

Substituting equations from (3) to (7) into (1) and (2), we get:

$$m_s \times \ddot{z}_s = K_S \times (z_u - z_s) + K_D \times (\dot{z}_u - \dot{z}_s) + F_A \tag{8}$$

$$m_u \times \ddot{z}_u = K_T \times (z_r - z_u) - K_S \times (z_u - z_s) - K_D \times (\dot{z}_u - \dot{z}_s) - F_A \tag{9}$$

The actuating force of the actuator, F_A, is generated by the pressure difference between the chambers inside the hydraulic cylinder (Fig. 1). Therefore, it is determined by equation (10).

$$F_A = S_P \times \Delta P \tag{10}$$

The variation of fluid pressure between chambers is a complex function that depends on the fluid flow. According to [16], this value is defined as follows:

$$\Delta P = \frac{1}{C_t} \times \left[C_d \times w \times x_{sv} \left(\frac{\left(P_0 - \Delta P \times sgn(x_{sv})\right)}{\rho} \right)^{\frac{1}{2}} - \frac{V \times \Delta \dot{P}}{4 \times \beta} - S_P \times (\dot{z}_s - \dot{z}_u) \right] \quad (11)$$

The displacement of the servo valve, x_{sv}, plays an essential role in changing the fluid pressure between chambers. This displacement depends on the control signal supplied by the controller, $i(t)$.

$$x_{sv} = -\tau \times \dot{x}_{sv} + k_{sv} \times i(t) \quad (12)$$

where:
S_P – Piston cross-sectional area, m^2
ΔP – Pressure difference, N/m^2
C_t – Leakage coefficient
C_d – Discharge coefficient
w – valve area gradient coefficient
ρ – hydraulic oil density, kg/m^3
V – Cylinder effective volume, m^3
P_0 – Initial pressure, N/m^2
β – Fluid bulk module, N/m^2
τ – Time coefficient, s
k_{sv} – servo valve coefficient, m/A

Combining (10), (11), and (12), we get an approximate linear equation (13) (see [33, 40]).

$$\dot{F}_A = \alpha_1 \times i(t) - \alpha_2 \times F_A + \alpha_3 \times (\dot{z}_u - \dot{z}_s) \quad (13)$$

with α_i are the coefficients of equation the (13).

Let $e(t)$ be the error between the output signal $y(t)$ and the reference signal $y_{ref}(t)$.

$$e(t) = y_{ref}(t) - y(t). \quad (14)$$

The purpose of the control is to make the value of error approaches zero, that is:

$$|e(t)| \xrightarrow{Minimum} 0. \quad (15)$$

As suggested above, this study uses a traditional PID control algorithm to eliminate the error $e(t)$ when the car oscillates. The PID algorithm has three stages corresponding to three functions: proportional, integral, and derivative. Therefore, the final control signal is synthesized from these three components.

$$i(t) = k_P \times e(t) + k_I \times \int e(t)dt + k_D \times \frac{de(t)}{dt}. \quad (16)$$

In the equation (16), the coefficients k_P, k_I, and k_D play an important role in ensuring the controller's performance. Many methods are used to find the optimal values for these coefficients (described in the previous section). However, optimal values are fixed in all cases. In fact, these values are only suitable for some instances, not all. Therefore, it is necessary to flexibly tune the controller coefficients to suit each vehicle's movement conditions. In this paper, a fuzzy algorithm is used to adjust the coefficients of the PID controller. Unlike previous studies, this fuzzy algorithm has an asymmetrical form. This aims to ensure that vehicle body displacement and acceleration are as minimal as possible.

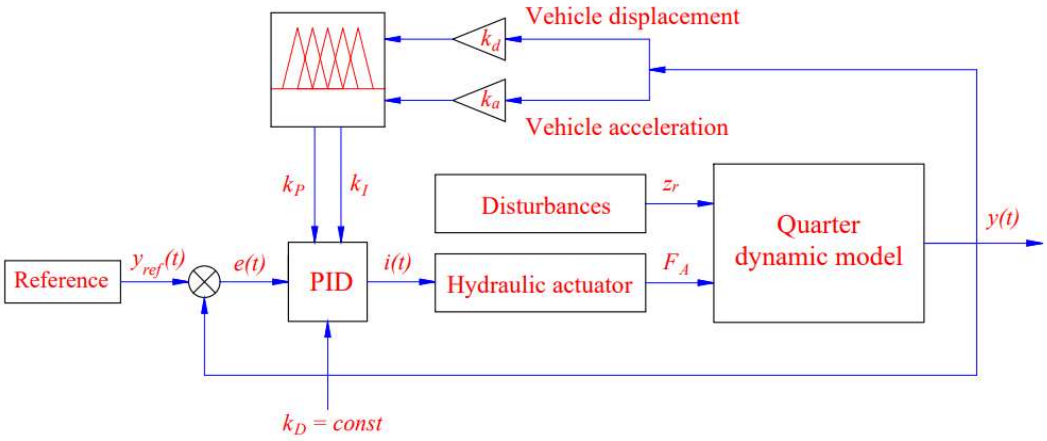

Fig. 2. Control system diagram.

The control system diagram is illustrated in Figure 2. According to this description, the values of the coefficients k_P and k_I are flexibly adjusted by the fuzzy algorithm, while the value of the k_D coefficient is unchanged (this is because the k_D coefficient is extremely sensitive, so it should be chosen within a small range). The fuzzy algorithm used in this study has two inputs: vehicle body displacement (the first input) and vehicle body acceleration (the second input). These two parameters can be obtained with sensors on the vehicle's body. They are multiplied by gain coefficients (k_d and k_a) before becoming the formal input of the fuzzy algorithm.

Figure 3 depicts the membership function of the coefficient k_P, while Figure 4 gives information about the membership function of the coefficient k_I. In Figure 3, we use trapezoidal membership functions with three levels: POS (positive), NEU (neutral), and NEG (negative). However, the membership function of the coefficient k_I, which is depicted in Figure 4, has seven steps: VLNEG (very large negative), LNEG (large negative), NEG (negative), NEU (neural), POS (positive), LPOS (large positive), and VLPOS (very large positive). Although the input ranges of these two membership functions are similar, the output variation is entirely different. For Figure 3, the output of the membership function changes only over a small range, while the output of Figure 4 changes continuously over a more extensive range.

The membership function of the proportional coefficient is designed so that its output value is always high, corresponding to each level. This helps control signal amplification when needed. Unlike k_P, the membership function of coefficient k_I is divided into more levels, which is suitable for different oscillation conditions. According to this idea, the system will not operate under minor oscillation conditions. In fact, the design of the membership function depends mainly on the perspective and experience of the researcher.

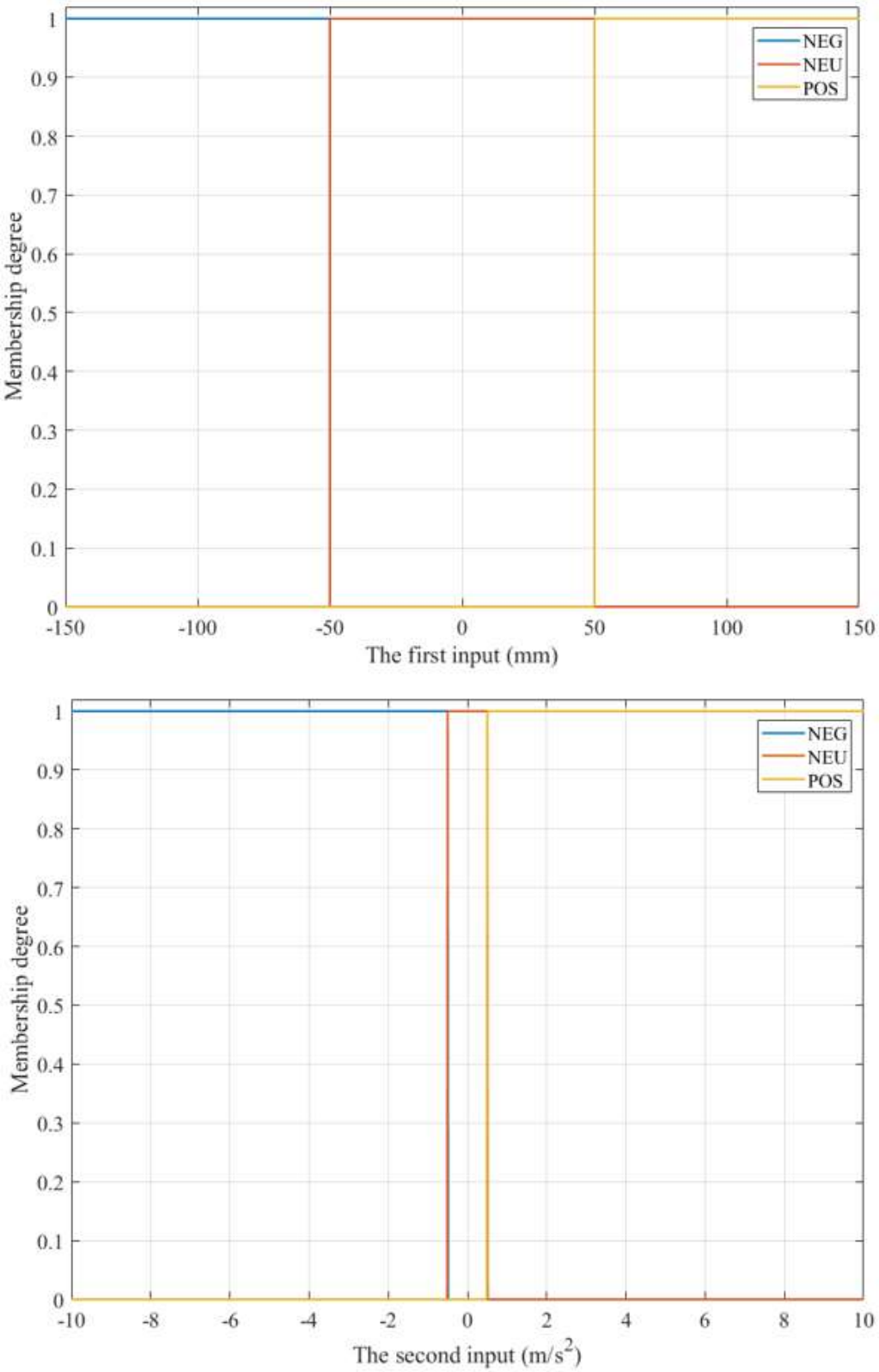

Fig. 3. Membership function (k_P coefficient).

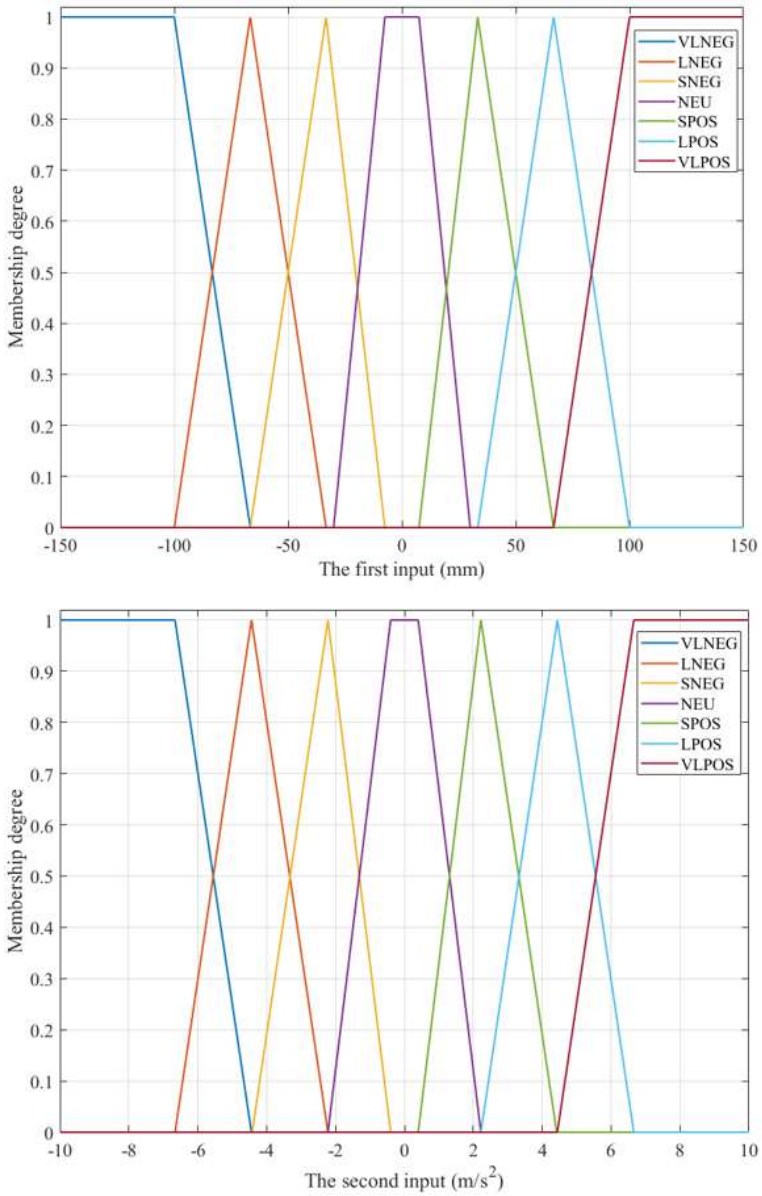

Fig. 4. Membership function (k_I coefficient).

The defuzzification process is performed based on the weighted sum (WTSUM) method, according to the equation (17).

$$y' = \beta_1 y_1 + \beta_2 y_2 + \cdots + \beta_m y_m = \sum_{i=1}^{m} w_i y_i = \gamma^T \Phi(x) \tag{17}$$

with:

$$w_i = \frac{\beta_i}{\sum_{i=1}^{m} \beta_i}, \qquad \gamma = \begin{bmatrix} y_1 \\ y_2 \\ y_3 \\ \dots \\ y_m \end{bmatrix}, \qquad \Phi(x) = \begin{bmatrix} w_1(x) \\ w_2(x) \\ w_3(x) \\ \dots \\ w_n(x) \end{bmatrix}.$$

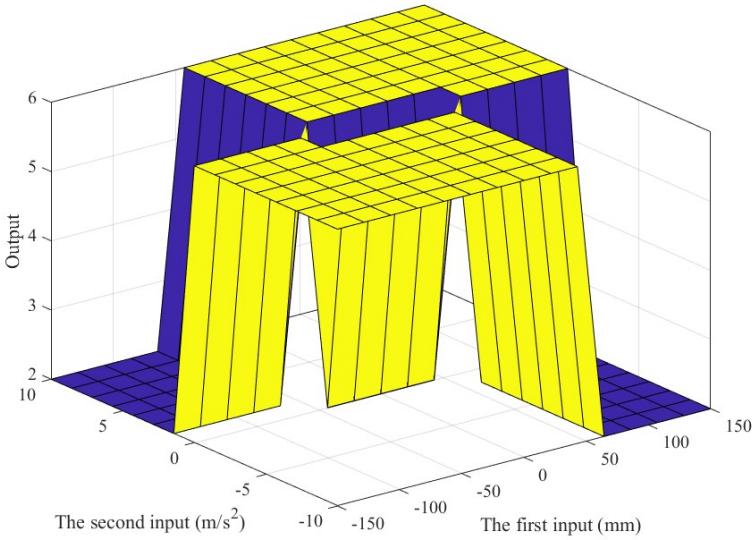

Fig. 5. Fuzzy surface (k_P coefficient).

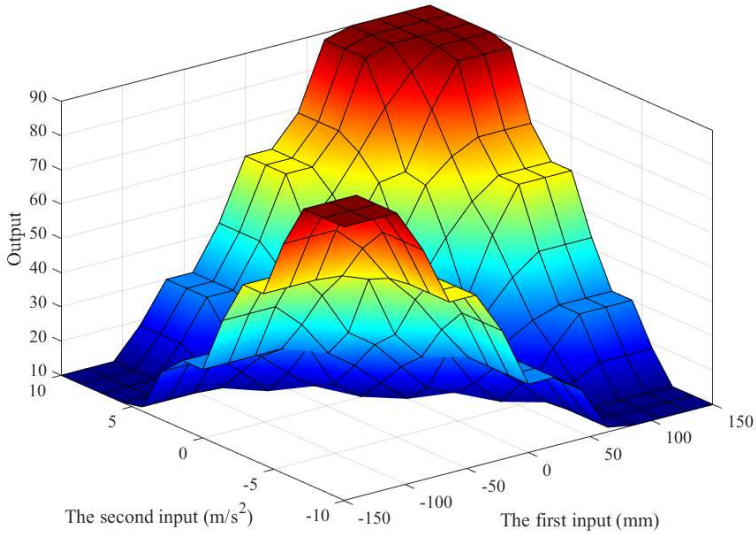

Fig. 6. Fuzzy surface (k_I coefficient).

Fuzzy rules are described in Table 1 (k_P coefficient) and Table 2 (k_I coefficient). These rules are plotted in Figures 5 and 6. As shown above, the fuzzy rule established in this study has an asymmetric form. This is a novelty of the paper compared to other studies.

Table 1. Fuzzy rules (k_P coefficient).

1st input	2nd input	Output
NEG	NEG	NEG
NEG	NEU	NEG
NEG	POS	NEU
NEU	NEG	NEG
NEU	NEU	NEU
NEU	POS	POS
POS	NEG	NEU
POS	NEU	POS
POS	POS	POS

Table 2. Fuzzy rules (k_I coefficient).

1st input	2nd input	Output	1st input	2nd input	Output
VLNEG	VLNEG	VLNEG	NEU	POS	POS
VLNEG	LNEG	LNEG	NEU	LPOS	POS
VLNEG	NEG	LNEG	NEU	VLPOS	LPOS

VLNEG	NEU	NEG	POS	VLNEG	NEG
VLNEG	POS	NEG	POS	LNEG	NEU
VLNEG	LPOS	NEU	POS	NEG	NEU
VLNEG	VLPOS	NEU	POS	NEU	POS
LNEG	VLNEG	LNEG	POS	POS	POS
LNEG	LNEG	LNEG	POS	LPOS	LPOS
LNEG	NEG	NEG	POS	VLPOS	LPOS
LNEG	NEU	NEG	LPOS	VLNEG	NEU
LNEG	POS	NEU	LPOS	LNEG	NEU
LNEG	LPOS	NEU	LPOS	NEG	POS
LNEG	VLPOS	POS	LPOS	NEU	POS
NEG	VLNEG	LNEG	LPOS	POS	LPOS
NEG	LNEG	NEG	LPOS	LPOS	LPOS
NEG	NEG	NEG	LPOS	VLPOS	VLPOS
NEG	NEU	NEU	VLPOS	VLNEG	NEU
NEG	POS	NEU	VLPOS	LNEG	POS
NEG	LPOS	POS	VLPOS	NEG	POS
NEG	VLPOS	POS	VLPOS	NEU	LPOS
NEU	VLNEG	NEG	VLPOS	POS	LPOS
NEU	LNEG	NEG	VLPOS	LPOS	VLPOS
NEU	NEG	NEU	VLPOS	VLPOS	VLPOS
NEU	NEU	NEU			

The process of calculation and numerical simulation will be carried out after completing the design of the control algorithm for the active suspension system.

3. RESULT AND DISCUSSION

3.1. Condition

Car vibrations are described in four cases, corresponding to the four types of excitations from the road surface (Figure 7). The first and second cases use time-varying cyclic excitation signals. The pulsed excitation signal is used in the third case, while the last case uses a random bump. The first and third cases have low frequencies, while the others have higher frequencies. In addition, these stimuli have large amplitudes except for the first case.

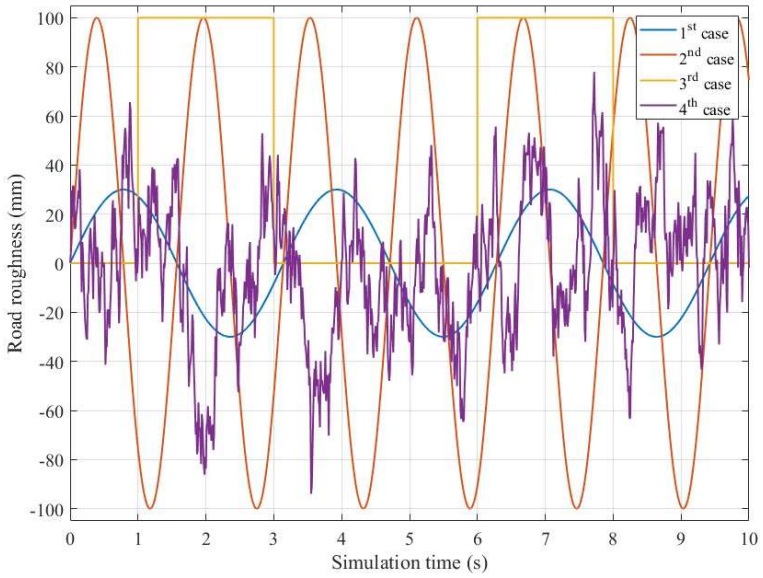

Fig. 7. Road roughness.

Numerical simulation is carried out with the MATLAB software. The parameters that are used for the calculation are referenced in Table 3. Three simulation situations are considered in each case: Hybrid PID, Traditional PID, and Passive. This aims to compare values obtained between situations, including maximum values and RMS values.

Table 3. Simulation parameters.

Symbol	Description	Value	Unit
K_S	Spring coefficient	43×10^3	N/m
K_T	Tire coefficient	3.8×10^3	N/m
K_D	Damping coefficient	176×10^3	Ns/m
m_s	Sprung mass	470	kg
m_u	Unsprung mass	48	kg
α_1	Hydraulic Actuator coefficient	539×10^3	$N^{3/2}/kg^{1/2}m^{1/2}V$
α_2	Hydraulic Actuator coefficient	1	1/s
α_3	Hydraulic Actuator coefficient	551×10^4	N/m

3.2. Simulation results

The first case:

According to Figure 7, the road bump in the first case has a sine waveform with a small amplitude and frequency. During the survey period (10 s), the amplitude of the stimulus signal did not exceed 30 mm. The change in body displacement is illustrated in Figure 8 with three situations: Hybrid PID, Traditional PID, and Passive. According to these results, the maximum displacement value when the car uses only mechanical suspension is 31.73 mm. The figures for the remaining situations are 16.65 mm and 7.58 mm, respectively, for Traditional PID and Hybrid PID. An evaluation of the RMS value of the displacement is necessary because this is a continuous oscillation. According to this criterion, the RMS values of three situations reach 22.19 mm, 11.54 mm, and 5.34 mm, respectively. When using a typical PID controller, the oscillation phase deviates slightly from the Passive situation. This phase difference is improved significantly once the Fuzzy-PID hybrid algorithm is applied.

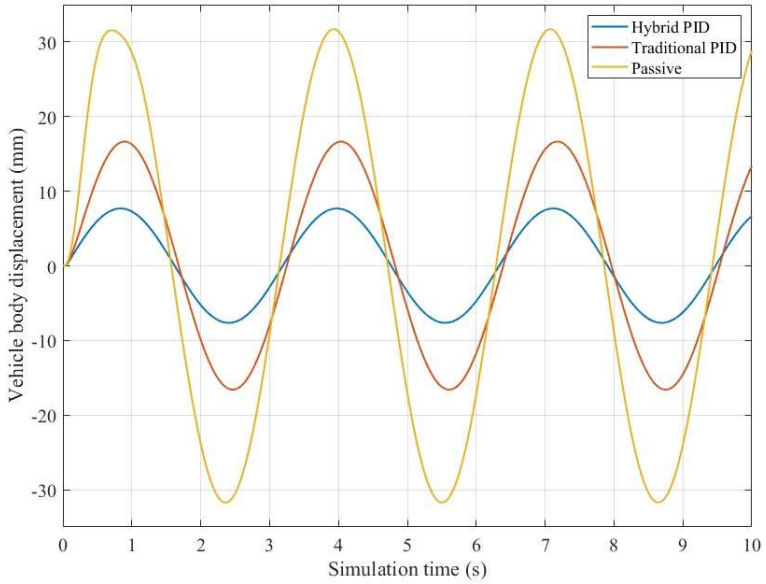

Fig. 8. Vehicle body displacement (the first case).

The change in body acceleration, in this case, is quite small (Figure 9). Their maximum values obtained from the simulation are 0.52 m/s^2, 0.32 m/s^2, and 0.27 m/s^2, respectively. These values are obtained at the first stage of the stimulation process. After that, they gradually decrease and oscillate steadily with a smaller amplitude. The phase difference between the signals still exists, but it is not too large. The RMS values obtained for all three scenarios are 0.11 m/s^2, 0.05 m/s^2, and 0.03 m/s^2, respectively.

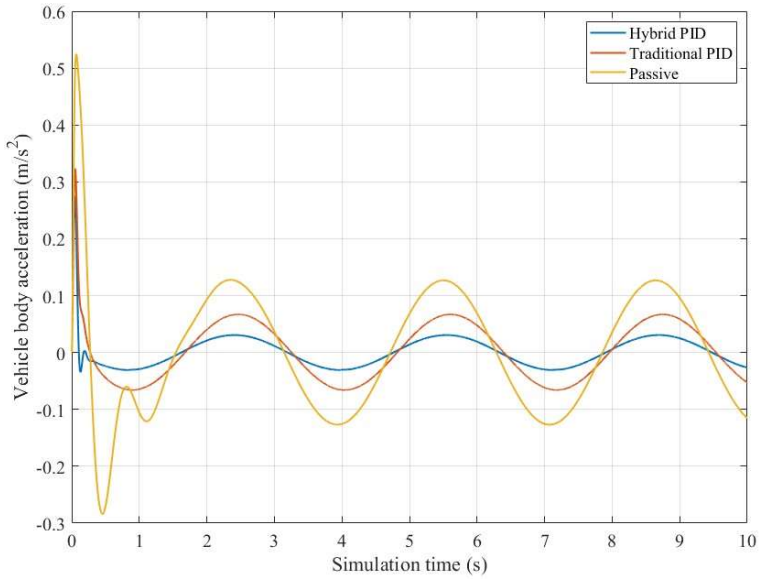

Fig. 9. Vehicle body acceleration (the first case).

The second case:

In the second case, the road excitation used remains a cyclic sine. However, the amplitude and frequency of the excitation signal are significantly enhanced. According to Figure 7, the peak amplitude of the excitation is up to 100 mm, while the frequency is 0.637 Hz. Therefore, the displacement of the vehicle body changes much more strongly than in the first case (Figure 10). According to the results obtained from the calculation process, the peaked displacement of the vehicle body can be up to 133.10 mm, corresponding to the RMS value of 76.48 mm. When using the active suspension system controlled by Traditional PID algorithm, these values drop sharply to 53.05 mm and 32.26 mm, respectively. In particular, if the Hybrid PID algorithm is used, these values are guaranteed to be stable (28.55 mm and 14.94 mm). In terms of applying Traditional PID algorithm, the phase difference occurs more strongly, while this is negligible when using the fuzzy algorithm to adjust the controller's parameters.

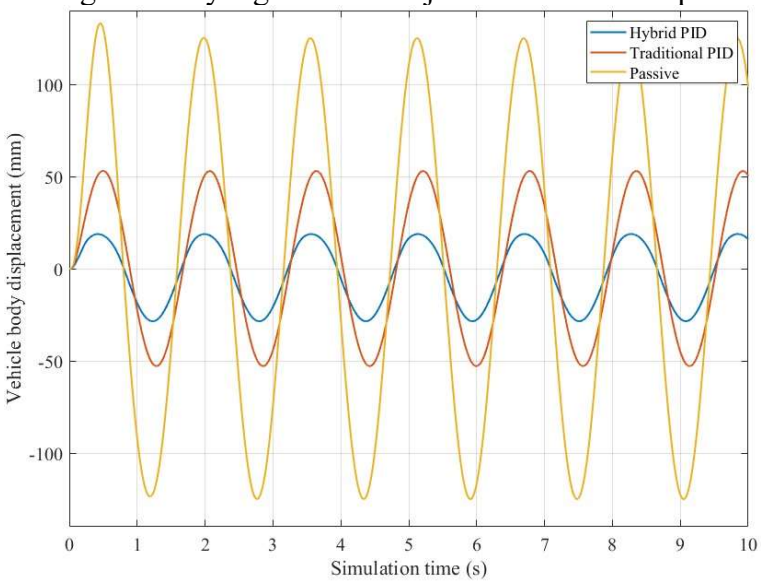

Fig. 10. Vehicle body displacement (the second case).

Similar to the first case, the vehicle acceleration in this case also peaks at the first phase of the oscillation. This value may be up to 3.46 m/s^2 if the car only uses the passive suspension system. Once a modern active suspension system is fitted, the maximum value of acceleration drops sharply to only 2.14 m/s^2 and 1.09 m/s^2, respectively, for Traditional PID and Hybrid PID. In subsequent phases, the vehicle body acceleration changes periodically with time, with

a smaller amplitude. There is a significant phase difference between two situations: Passive and Traditional PID. This is a significant limitation when using this algorithm to control the suspension system. Looking at Figure 11 more closely, we can see that the vehicle body's acceleration changes asymmetrically. This is because the fuzzy rule is chosen asymmetrically. This is a novelty in the study because it provides different results than previously published papers. This helps to ensure that the value of acceleration is small and does not cause a phase difference.

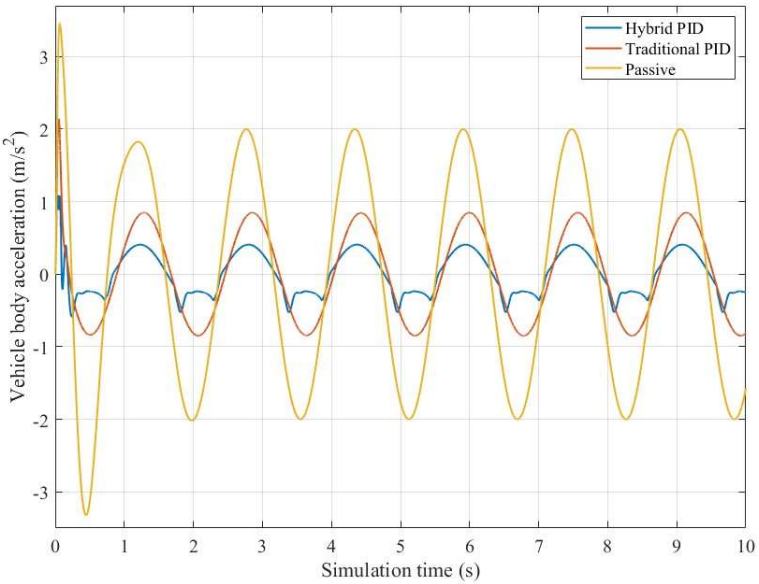

Fig. 11. Vehicle body acceleration (the second case).

The third case:

The third case uses a pulsed excitation signal with a height of 100 mm (Figure 7). The wheel is subject to sudden excitation. Therefore, the body is raised by a significant amount: 149.95 mm (Passive), 57.05 mm (Traditional PID), and 21.42 mm (Hybrid PID) (Figure 12). Because these are discontinuous excitation signals, we do not consider their RMS values.

The pulsed excitation signal causes a considerable acceleration of the vehicle body. This value increases suddenly to 23.76 m/s^2 when cars only use passive suspension. This value slightly decreases to 16.88 m/s^2 when applying Traditional PID algorithm to control the suspension system. In the case of using Hybrid PID algorithm, the peak value of acceleration declines sharply, reaching only 7.80 m/s^2 (Figure 13). These values decrease to zero after the stimulus ends. In two situations where the controller is used, these values may fluctuate briefly before returning to a stable position.

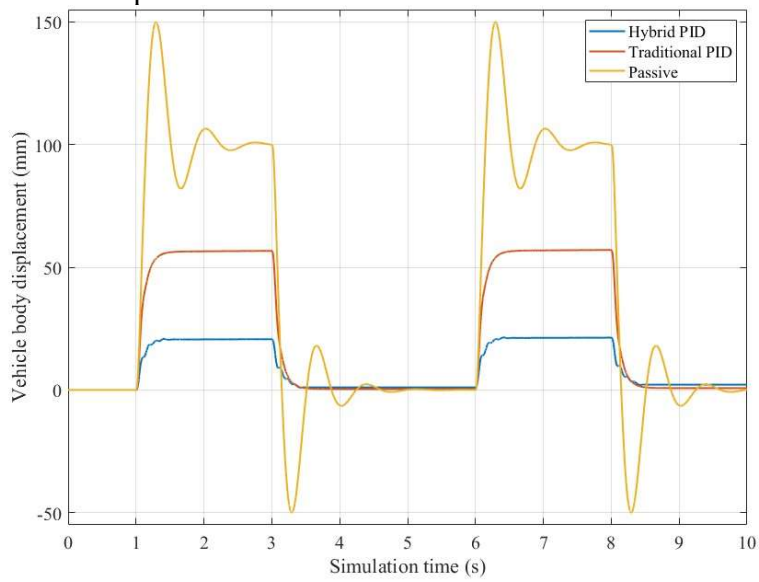

Fig. 12. Vehicle body displacement (the third case).

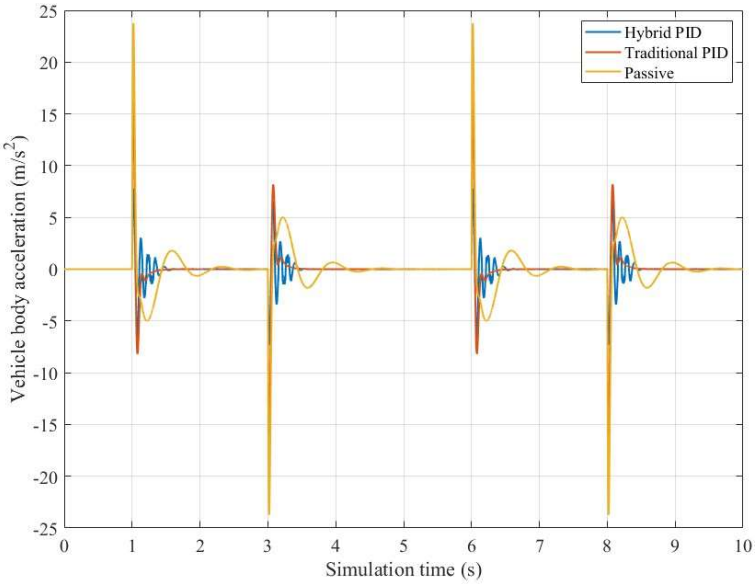

Fig. 13. Vehicle body acceleration (the third case).

The fourth case:

When the vehicle is traveling on the road, the wheels often encounter stimuli that take on a random form (Figure 7). These stimuli have significant frequencies and amplitudes, which vary continuously over time. According to Figure 14, the displacement of the vehicle body changes continuously and follows the stimulus signal of the road surface. The RMS values of three situations: Passive, Traditional PID, and Hybrid PID, reach 37.09 mm, 12.15 mm, and 6.19 mm, respectively, while their peak values are 109.37 mm, 38.19 mm, and 19.07 mm.

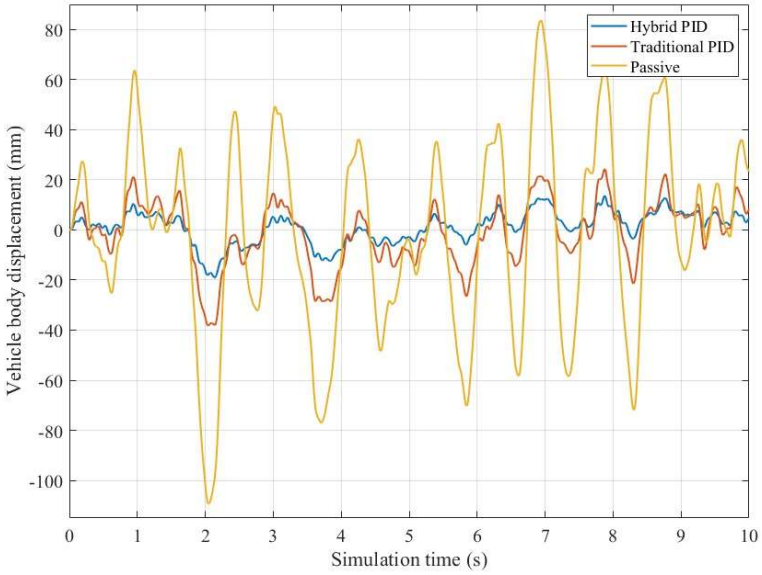

Fig. 14. Vehicle body displacement (the fourth case).

According to the results illustrated in Figure 15, the change in body acceleration over time is significant. The maximum acceleration of the body can be up to 13.68 m/s^2 if the automobile does not have the active suspension system. In contrast, this value is only 19.07 m/s^2 once the car is equipped with the active suspension system controlled by Hybrid PID algorithm.

In general, the active suspension helps to ensure more ride comfort than conventional mechanical suspension. The vehicle's smoothness can be improved when applying Traditional PID control algorithm. However, a significant phase difference occurs. If Hybrid PID algorithm is used, the values related to vehicle body displacement and acceleration can

decrease more sharply. Besides, the phase difference is also solved thoroughly. The hybrid algorithm, shown in this study, provides more performance than conventional algorithms.

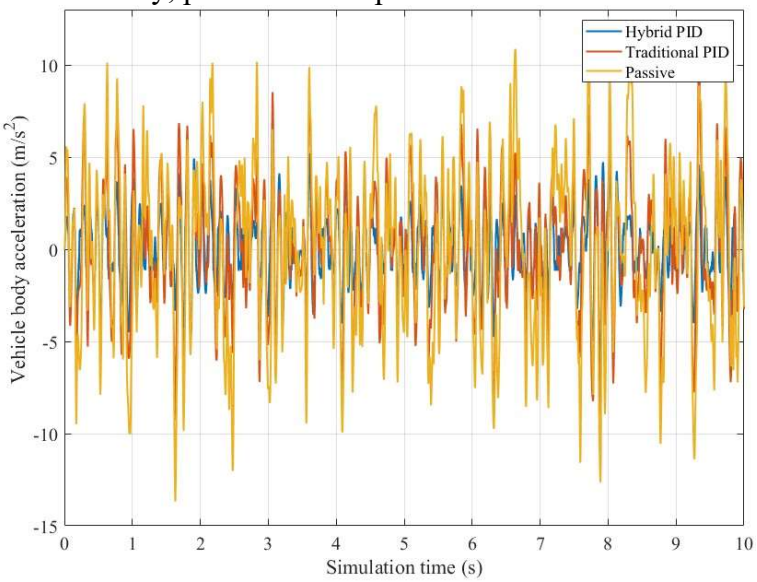

Fig. 15. Vehicle body acceleration (the fourth case).

Table 4 summarizes the results obtained from the simulation.

Table 4. Simulation results.

	Hybrid PID		Traditional PID		Passive	
The first case						
	Max	RMS	Max	RMS	Max	RMS
Displacement (mm)	7.68	5.34	16.65	11.54	31.73	22.19
Acceleration (m/s^2)	0.27	0.03	0.32	0.05	0.52	0.11
The second case						
	Max	RMS	Max	RMS	Max	RMS
Displacement (mm)	28.55	14.94	53.05	32.26	133.10	76.48
Acceleration (m/s^2)	1.09	0.56	2.14	1.03	3.46	1.91
The third case						
	Max	RMS	Max	RMS	Max	RMS
Displacement (mm)	21.42		57.05		149.96	
Acceleration (m/s^2)	7.80		16.88		23.76	
The fourth case						
	Max	RMS	Max	RMS	Max	RMS
Displacement (mm)	19.07	6.19	38.19	12.15	109.37	37.09
Acceleration (m/s^2)	6.30	1.55	10.27	2.76	13.68	4.20

4. CONCLUSION

The roughness of the road is the primary source of excitation, which causes car vibrations. Active suspension can control car vibrations more effectively than passive suspension. When evaluating vehicle smoothness, the maximum and RMS values of body displacement and acceleration should be taken into account.

In this study, we design a Hybrid PID controller to control the modern suspension system. This is a combination of conventional PID algorithms and fuzzy algorithms, allowing flexible controller parameter adjustment. The paper's results show that body displacement and acceleration values significantly decline when using the Hybrid PID algorithm in all four survey cases. In addition, the phase difference is negligible. In general, the smoothness of the vehicle body has been more guaranteed when applying this new algorithm. In this work, some problems still exist and cannot be resolved, including: 1) the change of acceleration is not smooth sufficient (the second case); 2) the convergence of displacement is not fast sufficient

(the third case); and 3) the effects of disturbances have not been fully mentioned. These will be addressed in future work.

REFERENCES

[1] Wu, L., Zhao, D., Zhao, X., & Qin, Y. (2020). Nonlinear Adaptive Back-Stepping Optimization Control of the Hydraulic Active Suspension Actuator, *Processes*, **11**(7), https://doi.org/10.3390/pr11072020

[2] Yoon, D. S., Kim, G. W. & Choi, S. B. (2021). Response time of magnetorheological dampers to current inputs in a semi-active suspension system: Modeling, control and sensitivity analysis, *Mechanical Systems and Signal Processing*, **146**, https://doi.org/10.1016/j.ymssp.2020.106999

[3] Zhao, R., et al. (2020). Adaptive vehicle posture and height synchronization control of active air suspension systems with multiple uncertainties, *Nonlinear Dynamics*, **99**, 2109–2127, https://doi.org/10.1007/s11071-019-05412-9

[4] Pan, H. & Sun, W. (2019). Nonlinear Output Feedback Finite-Time Control for Vehicle Active Suspension Systems, *IEEE Transactions on Industrial Informatics*, **15**(4), 2073–2082, https://doi.org/10.1109/TII.2018.2866518

[5] Kilicaslan, S. (2018). Control of active suspension system considering nonlinear actuator dynamics, *Nonlinear Dynamics*, **91**, 1383–1394, https://doi.org/10.1007/s11071-017-3951-x

[6] Jeong, Y., Sohn, Y., Chang, S., & Yim, S. (2022). Design of Static Output Feedback Controllers for an Active Suspension System, *IEEE Access*, **10**, 26948–26964, https://doi.org/10.1109/ACCESS.2022.3157326

[7] Manna, S., et al. (2022). Ant Colony Optimization Tuned Closed-Loop Optimal Control Intended for Vehicle Active Suspension System, *IEEE Access*, **10**, 53735–53745, https://doi.org/10.1109/ACCESS.2022.3164522

[8] Nguyen, M. L., et al. (2022). Application of MIMO Control Algorithm for Active Suspension System: A New Model with 5 State Variables, *Latin American Journal of Solids and Structures*, **19**(2), https://doi.org/10.1590/1679-78256992

[9] Chen, S., Cai, Y., Wang, J. & Yao, M. (2018). A Novel LQG Controller of Active Suspension System for Vehicle Roll Safety, *International Journal of Control, Automation and Systems*, **16**, 2203–2213, http://dx.doi.org/10.1007/s12555-017-0159-2

[10] Wang, D., Zhao, D., Gong, M. & Yang, B. (2018). Research on Robust Model Predictive Control for Electro-Hydraulic Servo Active Suspension Systems, *IEEE Access*, **6**, 3231–3240, http://dx.doi.org/10.1109/ACCESS.2017.2787663

[11] Li, W., et al. (2019). Robust nonfragile H_∞ optimum control for active suspension systems with time-varying actuator delay, *Journal of Vibration and Control*, 25(18), 2435-2452. http://dx.doi.org/10.1177/1077546319857338

[12] Ovalle, L., Rios, H. & Ahmed, H. (2022). Robust Control for an Active Suspension System via Continuous Sliding-Mode Controllers, *Engineering Science and Technology, an International Journal*, **28**, https://doi.org/10.1016/j.jestch.2021.06.006

[13] Liu, Y. J. & Chen, H. (2021). Adaptive Sliding Mode Control for Uncertain Active Suspension Systems With Prescribed Performance, *IEEE Transactions on Systems, Man, and Cybernetics: Systems*, **51**(10), 6414–6422. https://doi.org/10.1109/TSMC.2019.2961927

[14] Wang, G., Chadli, M. & Basin, M. V. (2021). Practical Terminal Sliding Mode Control of Nonlinear Uncertain Active Suspension Systems With Adaptive Disturbance Observer,

IEEE/ASME Transactions on Mechatronics, **26**(2), 789–797, https://doi.org/10.1109/TMECH.2020.3000122.

[15] Pusadkar, U. S., Chaudhari, S. D., Shendge, P. D. & Phadke, S. B. (2019). Linear disturbance observer based sliding mode control for active suspension systems with non-ideal actuator, *Journal of Sound and Vibration*, 442, 428-444. https://doi.org/10.1016/j.jsv.2018.11.003

[16] Nguyen, D. N. & Nguyen, T. A. (2022). Evaluate the stability of the vehicle when using the active suspension system with a hydraulic actuator controlled by the OSMC algorithm, *Scientific Reports*, **12**, https://doi.org/10.1038/s41598-022-24069-w

[17] Nguyen, T. A. (2023). A New Approach to Selecting Optimal Parameters for the Sliding Mode Algorithm on an Automotive Suspension System, *Complexity*, https://doi.org/10.1155/2023/9964547

[18] Golouje, Y. N. & Abtahi, S. M. (2021). Chaotic dynamics of the vertical model in vehicles and chaos control of active suspension system via the fuzzy fast terminal sliding mode control, *Journal of Mechanical Science and Technology*, **35**(1), 31–43, https://doi.org/10.1007/s12206-020-1203-3

[19] Shaer, B., Kenne, J. P., Kaddissi, C., and Fallaha, C. (2018). A chattering-free fuzzy hybrid sliding mode control of an electrohydraulic active suspension, *Transactions of the Institute of Measurement and Control*, **40**(1), 222–238, https://doi.org/10.1177/0142331216652468

[20] Li, W., et al. (2019). Fuzzy finite-frequency output feedback control for nonlinear active suspension systems with time delay and output constraints, *Mechanical Systems and Signal Processing*, **132**, 315–334. https://doi.org/10.1016/j.ymssp.2019.06.018

[21] Xie, Z., et al. (2022). Dynamic-output-feedback based interval type-2 fuzzy control for nonlinear active suspension systems with actuator saturation and delay, *Information Sciences*, **607**, 1174–1194, https://doi.org/10.1016/j.ins.2022.06.055

[22] Mustafa, I. Y., Wang, H. P. & Tian, Y. (2019). Vibration control of an active vehicle suspension systems using optimized model-free fuzzy logic controller based on time delay estimation, *Advances in Engineering Software*, **127**, 141–149, https://doi.org/10.1016/j.advengsoft.2018.04.009

[23] Wang, H., Lu, Y., Tian, Y. & Christov, N. (2020). Fuzzy sliding mode based active disturbance rejection control for active suspension system, *Proceedings of the Institution of Mechanical Engineers, Part D: Journal of Automobile Engineering*, **234**(2–3), 449–457, https://doi.org/10.1177/0954407019860626

[24] Bongain, S. & Jamett, M. (2018). Electrohydraulic Active Suspension Fuzzy-Neural Based Control System, *IEEE Latin America Transaction*, **16**(9), 2454–2459, https://doi.org/10.1109/TLA.2018.8789568

[25] Chao, C. T., Liu, M. T., Wang, C. J. & Chiou, J. S. (2020). A fuzzy adaptive controller for cuckoo search algorithm in active suspension system, *Journal of Low Frequency Noise, Vibration and Active Control*, **39**(3), 761–771, https://doi.org/10.1177/1461348418811473

[26] Zahra, A. K. A. & Abdalla, T. Y. (2021). Design of Fuzzy Super Twisting Sliding Mode Control Scheme for Unknown Full Vehicle Active Suspension Systems Using an Artificial Bee Colony Optimization Algorithm, *Asian Journal of Control*, **23**(4), 1966–1981, https://doi.org/10.1002/asjc.2352

[27] Mohammadikia, R. & Aliasghary, M. (2019). Design of an interval type-2 fractional order fuzzy controller for a tractor active suspension system, *Computers and Electronics in Agriculture*, **167**, https://doi.org/10.1016/j.compag.2019.105049

[28] Lin, B., Su, X. & Li, X. (2019). Fuzzy sliding mode control for active suspension system with proportional differential sliding mode observer, *Asian Journal of Control*, **21**(1), 264–276, https://doi.org/10.1002/asjc.1882

[29] Munawwarah, S. & Yakub, F. (2021). Control analysis of vehicle ride comfort through integrated control devices on the quarter and half car active suspension systems, *Proceedings of the Institution of Mechanical Engineers, Part D: Journal of Automobile Engineering*, **235**(5), 1256–1268, https://doi.org/10.1177/0954407020968300

[30] Nguyen, D. N. & Nguyen, T. A. (2022). A Hybrid Control Algorithm Fuzzy-PI with the Second Derivative of the Error Signal for an Active Suspension System, *Mathematical Problems in Engineering*, https://doi.org/10.1155/2022/3525609

[31] Khodadadi, H. & Ghadiri, H. (2018). Self-tuning PID controller design using fuzzy logic for half car active suspension system, *International Journal of Dynamics and Control*, **6**, 224–232, https://doi.org/10.1007/s40435-016-0291-5

[32] Nguyen, D. N. & Nguyen, T. A. (2023). Proposing an original control algorithm for the active suspension system to improve vehicle vibration: Adaptive fuzzy sliding mode proportional-integral-derivative tuned by the fuzzy (AFSPIDF), *Heliyon*, **9**(3), https://doi.org/10.1016/j.heliyon.2023.e14210

[33] Nguyen, T. A. (2023). A novel approach with a fuzzy sliding mode proportional integral control algorithm tuned by fuzzy method (FSMPIF), *Scientific Reports*, **13**, https://doi.org/10.1038/s41598-023-34455-7

[34] Swethamarai, P. & Lakshmi, P. (2022). Adaptive-Fuzzy Fractional Order PID Controller-Based Active Suspension for Vibration Control, *IETE Journal of Research*, **68**(5), 3487–3502, https://doi.org/10.1080/03772063.2020.1768906

[35] Liu, J., Li, X., Zhang, X. & Chen, X. (2019). Modeling and Simulation of Energy-Regenerative Active Suspension Based on BP Neural Network PID Control, *Shock and Vibration*, https://doi.org/10.1155/2019/4609754

[36] Li, M., Li, J., Li, G. & Xu, J. (2022). Analysis of Active Suspension Control Based on Improved Fuzzy Neural Network PID, *World Electric Vehicle Journal*, **13**(12), https://doi.org/10.3390/wevj13120226

[37] Nguyen, T. A. (2023). Design a new control algorithm AFSP (Adaptive Fuzzy – Sliding Mode – Proportional – Integral) for automotive suspension system, *Advances in Mechanical Engineering*, **15**(2), https://doi.org/10.1177/16878132231154189

[38] Mahmoodabadi, M. J. & Nejadkourki, N. (2022). Optimal fuzzy adaptive robust PID control for an active suspension system, *Australian Journal of Mechanical Engineering*, **20**(3), 681–691, https://doi.org/10.1080/14484846.2020.1734154

[39] Talib, M. H. A., et al. (2023). Experimental evaluation of ride comfort performance for suspension system using PID and fuzzy logic controllers by advanced firefly algorithm, *Journal of the Brazilian Society of Mechanical Sciences and Engineering*, **45**, https://doi.org/10.1007/s40430-023-04057-5

[40] Nguyen, T. A. (2021). Advance the Efficiency of an Active Suspension System by the Sliding Mode Control Algorithm With Five State Variables, *IEEE Access*, **9**, 164368–164378, https://doi.org/10.1109/ACCESS.2021.3134990

